STABILITY ANALYSIS AND OPTIMAL CONTROL DESIGN FOR AC-DC POWER SYSTEM WITH CONSTANT POWER LOAD

by

Jean-Marc Coulomb

B.S. in Electrical Engineering, ESIGELEC, 2011

Submitted to the Graduate Faculty of

the Swanson School of Engineering in partial fulfillment

of the requirements for the degree of

Master of Science

University of Pittsburgh

2012

UNIVERSITY OF PITTSBURGH

SWANSON SCHOOL OF ENGINEERING

This thesis was presented

by

Jean-Marc Coulomb

It was defended on

November 16th 2012

and approved by

Zhi-Hong Mao, Ph.D., Associate Professor, Department of Electrical and Computer Engineering

Mahmoud El Nokali, Ph.D., Associate Professor, Department of Electrical and Computer Engineering

George Kusic, Ph.D., Associate Professor, Department of Electrical and Computer Engineering

Gregory Reed, Ph.D., Associate Professor, Department of Electrical and Computer Engineering

Thesis Advisors: Zhi-Hong Mao, Ph.D., Associate Professor, Department of Electrical and Computer Engineering,

& Dr. Gregory Reed, Ph.D., Associate Professor, Department of Electrical and Computer Engineering

STABILITY ANALYSIS AND OPTIMAL CONTROL DESIGN FOR AC-DC POWER SYSTEM WITH CONSTANT POWER LOAD

Jean-Marc Coulomb, M.S.

University of Pittsburgh, 2012

This thesis studies the stability properties of an AC-DC system - a three-phase controlled rectifier - with constant power load (CPL) and proposes an optimal design for the system control. CPLs have been widely seen in power electronic applications. For example, motor drives and DC/AC inverters in advanced automotive systems may behave as CPLs. Due to their negative impedances, CPLs often impact the power quality and stability of an AC/DC system. This thesis considers a typical AC/DC system with constant power load, where the three-phase rectifier is originally controlled by two PI controllers. It is demonstrated that the PI control strategy obtains narrow stability margin. To overcome the limitation of PI control, a linear quadratic regulator with full state feedback is used to determine the optimal structure of the controller and tune the parameters of the controller and DC filter. This method is shown to improve the stability margin of the AC-DC system tremendously.

TABLE OF CONTENTS

LIST OF FIGURES

1.0 INTRODUCTION

1.1 STATEMENT

Power electronics are involved in many applications. The number of applications has been growing significantly during the last decades.

Among those applications, there is a typical type of load: the constant power load (CPL). This type of load has always been an important issue both for the industry and for researchers. Indeed, the constant power load exhibits unique characteristics and dynamics due to their negative impedance characteristic.

Many studies have been performed on the constant power loads since they can be encountered in many different areas. Let us mention, for example, a load fed by a motor, by a converter, or even a load in a microgrid.

This type of load is completely different from the regular loads. Indeed, the constant power load has a stability issue that can significantly degrade the stability of the system. As mentioned, several studies have been performed on this topic but there is still no generalized solution. However, it is totally possible to stabilize a particular system using a specific control method. Additional investigations need to be done to strictly establish the stability limits and obtain more accurate models.

In this study, the model consists in a constant power load fed by a three-phase controlled rectifier.

1.2 OBJECTIVES

The main purpose of this study is to find the stability limits of a given system and to apply an optimal control method on it to enhance these limits.

As it was mentioned previously, the system is a three-phase controlled rectifier feeding a constant power load. It is of interest to study the behaviors of the system with given parameters. Another interesting study to do is to slightly change the value of some of the parameters and observe the system's reactions. Some parameters will affect the stability limits while others will not.

As mentioned, the main purpose is to improve the system's stability. To achieve this goal, an optimal control method will be applied: Linear Quadratic Regulator method (LQR).

This method will considerably increase the system's stability limits. However, since this study is strictly theoretical and there are no specific design requirements, it will then be impossible to determine new fixed limits for the system's stability.

1.3 LAYOUT

This study is composed of four chapters:

- Chapter one - Literature review

  This chapter introduces the state-of-art with a literature review. It begins with various explanations and examples about the constant power load issue. It clearly explains why constant power load is a recurrent problem for the global stability of the system by giving several examples that it is likely to encounter. Then, the following part will be a complete review of what it has been done in this area and see what kind of control methods have been applied to make the system more stable.

- Chapter two - Description of the system

  This chapter develops the main problem of the study. It introduces the model, the controllers' schematic and the different control loops.

- Chapter three - Solution

  This chapter develops the solution that was chosen to enhance the stability of the system. The different methods to derive a model into a matrix form are briefly introduced and explained. The following step is the derivation of the model using the dq-transformation method. The equations of the controllers are also derived. Then, Kirchhoffs' voltage and current laws are applied to derive the equations of the dq-transformed model and the resulting set of equations is linearized in order to be put in matrix form. The next step is to calculate the coefficients' values of the PI (Proportional Integral) controllers using the Classical method. Finally, the use of the Linear Quadratic Regulator method applied on the system is explained.

- Chapter four - Simulations and results

  This chapter describes the different simulations made. The stability limits of the original system are determined and the effects of the change in some parameters values are investigated. The different results are shown for the system excited by a step.

2.0 LITERATURE REVIEW

2.1 GENERAL POINTS

Power converters are involved in a wide range of applications including electric motor drivers, power supply, harmonic and reactive power compensators in transmission lines, telecommunication [2], [3], [4], [5], [6], naval ships [7], or industrial power systems [8], [9], [10]. Of course, this list is non-exhaustive. For most of those applications, the load is modeled as a resistor, a constant source, or a series combination of voltage source, resistor or inductor. However, another type of load which is called constant power load is commonly encountered [11].

The stability of the constant power loads is a recurrent problem. It represents an important issue, especially when feeding electric machines. This type of load can significantly degrade the stability of the system. Consequently, studies need to be performed in order to improve the behaviors of those systems.

Actually, the number of studies done on stability and behaviors of systems feeding a constant power load is relatively small. Several methods have been applied to stabilize specific systems, but none can be generalized. It would also be interesting to get more details in order to obtain more accurate models. In other words, we still do not have a full understanding of this problem, mainly because of the unique characteristics and dynamics of the constant power load.

Let us take the example of an electric motor fed by a constant power load which appears to be very frequent [12], [13]. When the motor is tightly controlled, it behaves as a constant power load.

Figure [1] represents a constant power load fed by a motor.

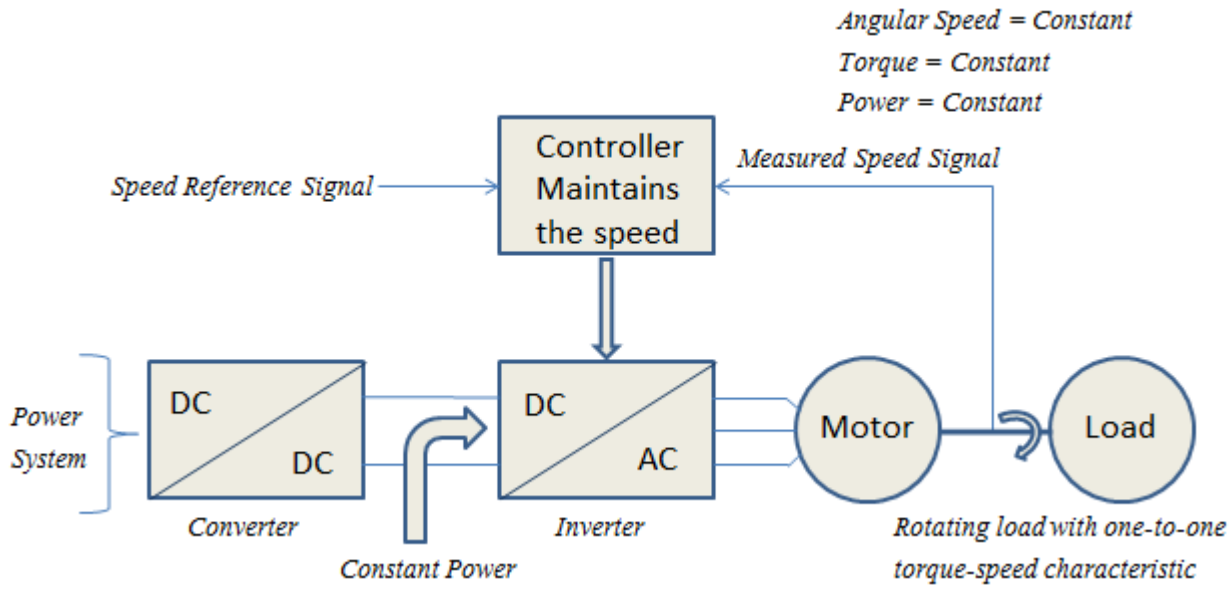

Figure 1: Electric motor feeding a constant power load

Let us assume that the controller tightly regulates the speed. Therefore, the motor has a one-to-one linear torque-speed characteristic. Equation (2.1) shows the relation between power, torque and angular speed.

$$P = T \times \Omega \tag{2.1}$$

The speed is constant since it is regulated by the controller. The motor has a one-to-one torque-speed relation, so for each speed there is a corresponding torque. This means that the torque is also constant. According to equation (2.1), the power which is the product of the torque and the angular speed is also constant.

Moreover, if we assume a constant efficiency, it can be ensured that the input power is also constant. Consequently, the system exhibits constant power load characteristics.

Figure [2] represents the most basic circuit involving a constant power load [12]. In this case, the type of converter is DC/DC and the load is a resistor. A resistor exhibits a linear voltage-current relation.

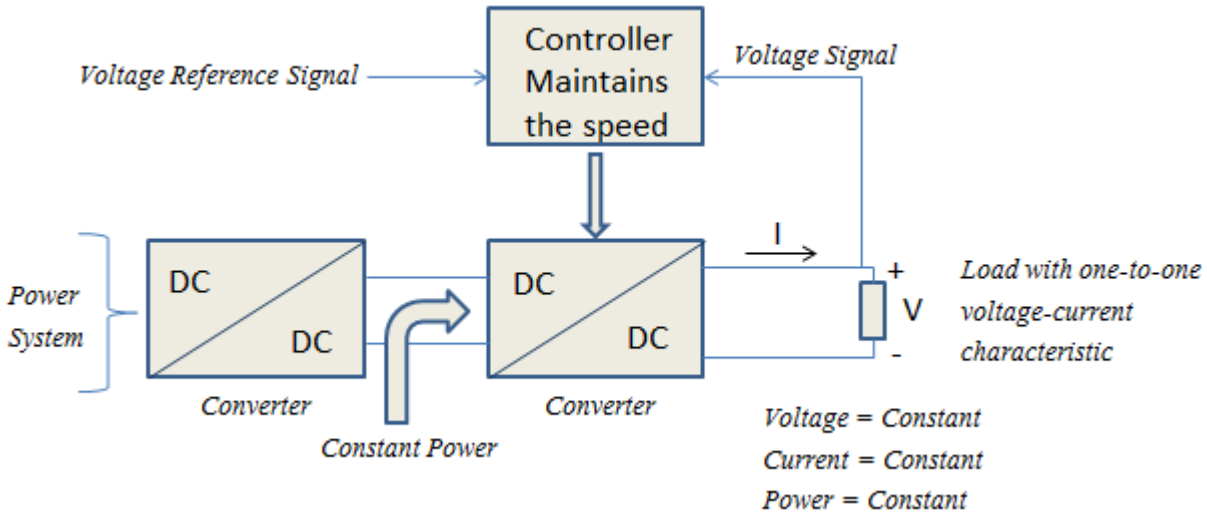

Figure 2: DC/DC converter feeding a constant power load

The main idea is similar to the one from the previous example. The value of the resistor is fixed. The controller tightly regulates the value of the voltage in order to keep it constant. Equation (2.2) shows the relation between current and voltage for this circuit.

$$I = V \times R \tag{2.2}$$

As a consequence, the current remains constant too. Finally, the power can be obtained by equation (2.3)

$$P = V \times I \tag{2.3}$$

Then, the power is also constant.

It has been mentioned earlier in this study that the cause of this instability comes from the negative impedance characteristic. Let us highlight in equation (2.4) that the instantaneous impedance is always positive.

$$\frac{V}{I} > 0 \tag{2.4}$$

On the other hand, the incremental impedance, which can be represented as the overall impedance, is always negative as shown in equation (2.5).

$$\frac{dV}{dI} < 0 \tag{2.5}$$

The incremental impedance is shown in figure [3].

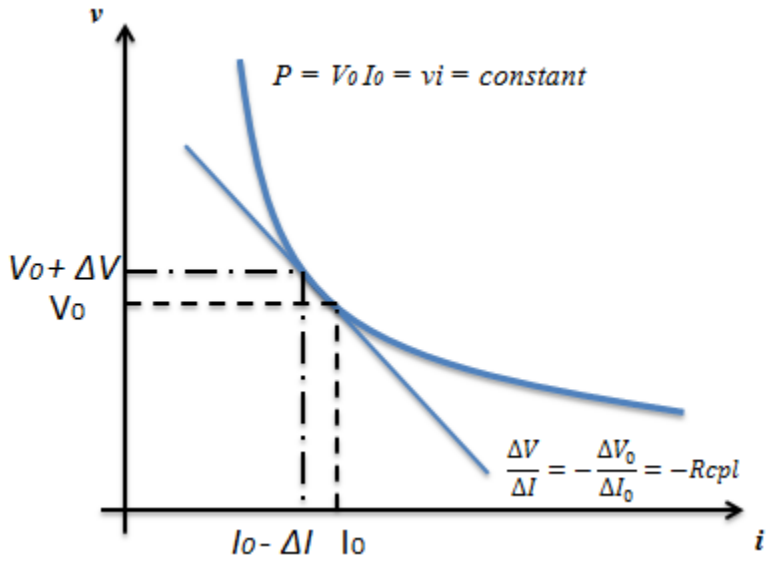

Figure 3: Voltage-current curve of a constant power load

Let us now consider figure [3]. The negative impedance characteristic has a negative influence on the power quality and on the global stability of the system. This effect is simply called the negative impedance instability. The negative impedance characteristic is represented as a curve with a negative slope. In other words, it means that when the voltage increases, the current decreases for a same amount of power. And vice-versa, if the current

increases, the voltage decreases. Equation (2.6) shows the calculation of the incremental resistance of a constant power load.

$$R_{cpl} = (\frac{\partial i}{\partial v})^{-1} = \frac{-V^2}{P} \tag{2.6}$$

According to equation (2.3) and since the power is constant, it can easily be observed that if the value of one of the two parameters changes, the other one has to adjust. This is the core of the problem.

Let us come back to the previous statement: if the current decreases, the voltage increases. This will lead the current to decrease even more. Therefore, the system becomes completely unstable.

Figure [4] represents another example of this negative impedance instability issue and it is interesting to explain it with further details.

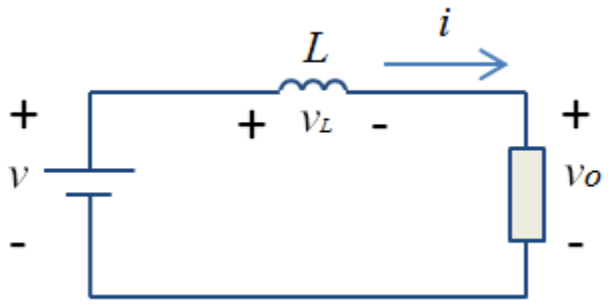

Figure 4: DC source feeding a constant power load through an inductor

Figure [4] is a simple circuit that includes a DC power source, an inductor L and a load connected in series. Equation (2.7) shows the output power of the circuit represented in figure [4].

$$P = v_0 \times i_0 = Constant \tag{2.7}$$

It is interesting to examine the circuit's behaviors because of the negative impedance issue.

First, let us establish the position of the equilibrium point. The equilibrium point can be reached with the voltage source equal to the voltage load. Operating at the equilibrium point means that we are in steady state. Let us now compare the two voltage-current curves of the system and see how the equilibrium point behaves.

Figure [5] represents the voltage-current characteristic of a basic voltage source and a constant power load.

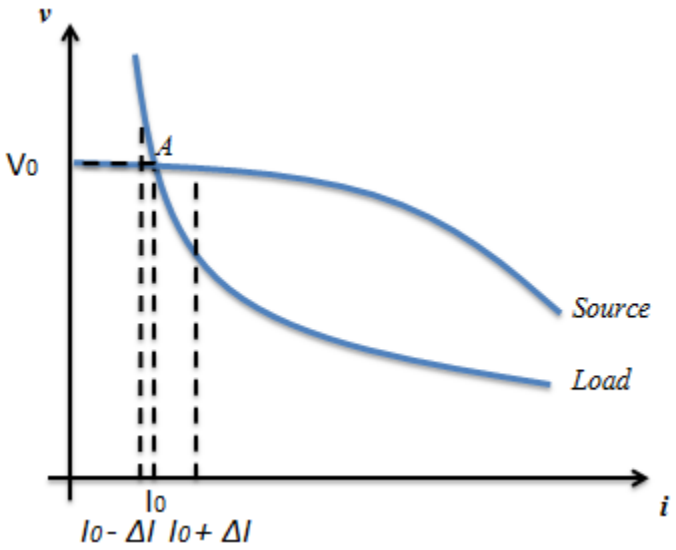

Figure 5: Voltage-current characteristics of a voltage source and a constant power load

The equilibrium point is represented by point A and is located at the intersection of the two curves. To have a better understanding, it must be mentioned that the system is considered stable if it returns to the equilibrium point after a disturbance. In other words, it has to converge towards its original state. If it does not, it is considered as an unstable system. The disturbance may appear either in the source or in the load.

Let us now fully analyze the behaviors of figure [5]. To begin, let us assume a disturbance which causes a reduction in the current of Δi. According to figure [5], it can be noticed that the load voltage is now larger than the source one. As a consequence, the current decreases further since the source voltage becomes smaller. Therefore, the operating point moves away from the equilibrium point A. Finally, the current reaches zero while the voltage reaches infinity.

A similar phenomenon occurs when the current increases after a small perturbation. The load voltage becomes smaller than the source voltage. This means that the current increases even more. Again, the operating point moves away from its initial position. Similarly, the current reaches infinity while the voltage goes to zero.

It is now clear that point A is an unstable point of equilibrium. There is no way that the system can be stable after a disturbance without control. It should be mentioned that the system acts as a positive feedback.

To compare the constant power load system with a regular system, let us replace the constant power load by a resistor. The source and the inductor remain the same. Figure [6] represents the voltage-current characterestics of both the voltage source and the resistive load.

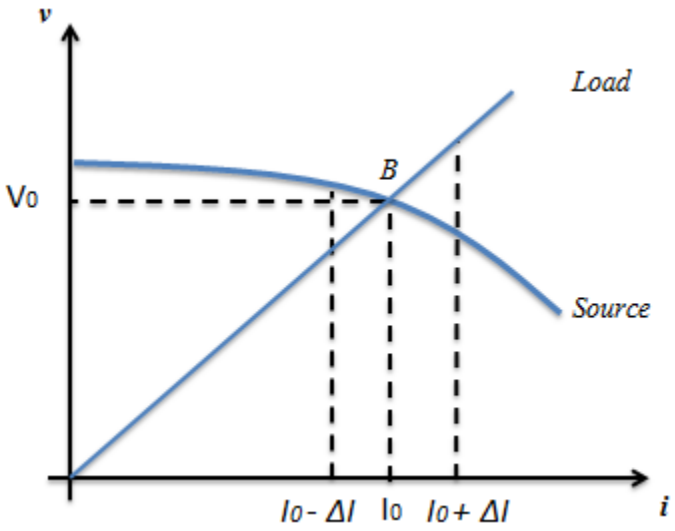

Figure 6: Voltage-current characteristics of a voltage source and a resistive load

Similarly to the previous study, let us examine how the equilibrium point B moves and check whether the system is stable or not. To begin, let us remind the difference between the two loads: the constant power load exhibits a negative incremental impedance while the resistor exhibits a positive incremental impedance.

Let us use the same procedure to study the system. Assume a perturbation that de-

creases the current of a value of Δi. The load voltage is now smaller than the source voltage. According to Kirchhoff's voltage law, the voltage called v_L across the inductance L is positive. Consequently, the current increases until it reaches its initial value. It returns to the equilibrium point.

On the other hand, if the current increases due to a disturbance, the load voltage becomes larger than the source voltage. According to Kirchhoff's voltage law, the voltage v_L across the inductor L is negative. The current decreases and the system returns to the initial state.

Therefore, the system is stable. After a disturbance, it returns to the equilibrium point. This system behaves as a negative feedback.

Reference [14] shows an interesting review of the different loads' characteristics. It basically says that loads are characterized by their voltage dependency as shown in equation (2.8).

$$P = P_0 \times (\frac{u}{u_0})^{MP} \tag{2.8}$$

In equation (2.8), P represents the power of the load, P_0 represents the initial power consumption, U is the voltage and U_0 is the initial voltage. Equation (2.8) is true for the smallest change in U.

The exponent MP represents the three main types of load:

- If $MP = 0$, the load power demand is independent of the voltage amplitude, then the load acts as a constant power load.
- If $MP = 1$, the load power demand is proportional to the voltage amplitude, then the load acts as a constant current load.
- If $MP = 2$, the load power demand is proportional to the square of the voltage amplitude, then the load acts as a constant impedance load (resistance load).

To illustrate, let us give the example of a rising voltage for each type of load. The current decreases for a constant power load, it does not change for a constant current load and it increases for a constant impedance load. Reference [15] provides additional information about the different types of load.

2.2 MODELING

Let us clarify the large-signal and small-signal models of a constant power load. These models can be encountered in many studies. Equation (2.9) represents the power of the constant power load at the operating point [16].

$$P_0 = v_0 \times i_0 \tag{2.9}$$

Let us now assume a small perturbation around this operating point, as shown in equations (2.10) and (2.11).

$$i_0 = I_0 + \widehat{i}_0 \tag{2.10}$$

$$v_0 = V_0 + \widehat{v}_0 \tag{2.11}$$

Equation (2.12) shows the result obtained after substituting equations (2.10) and (2.11) into (2.9).

$$P_0 = (V_0 + \widehat{v}_0) \times (I_0 + \widehat{i}_0) \tag{2.12}$$

And by neglecting the second-order term, the result becomes equation (2.13).

$$R_{cpl} = \frac{\widehat{v}_0}{\widehat{i}_0} = \frac{V_0}{I_0} = -R_0 \tag{2.13}$$

Equation (2.13) refers to the negative impedance characteristic for a small-signal model. Figure [7] represents the large-signal model while figure [8] shows the small-signal model.

The large-signal model is used to calculate the operating point while the small-signal model is used to determine the transfer function [16].

Consider the case of an uncontrolled rectifier or a converter with unity power factor ($\alpha = 1$), the constant power load can be represented as a pure negative resistance. On the other hand, with a power factor different from unity, a reactive element must be added in the

model [17]. The power factor is a phase difference between the voltage and the fundamental component of the current.

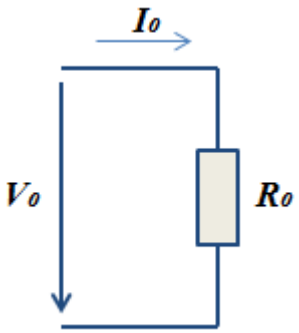

Figure 7: Large-signal model of a constant power load

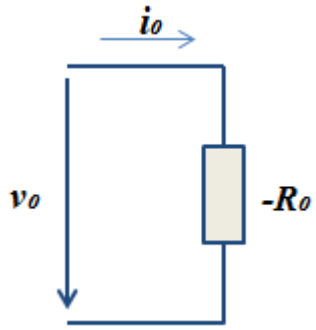

Figure 8: Small-signal model of a constant power load

Figure [9] represents the model with a unity power factor while figure [10] represents the model with a power factor different from unity.

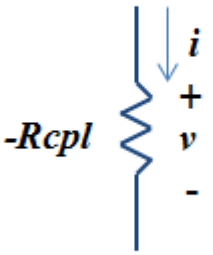

Figure 9: Converter with unity power factor

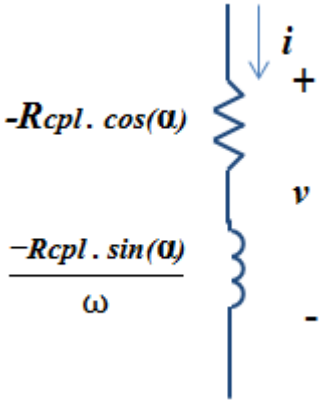

Figure 10: Converter with power factor different from unity

2.3 CONTROL METHODS

It is important to mention that because of the non-linearity, time-dependency and negative impedance characteristic of the converters and loads, the classical linear control meth-

ods show limitations when the behaviors are considered [12]. Therefore, stabilizing control methods must be used to ensure large-signal stability [18], [19], [20], [21], [22].

The authors of reference [20] studied the behaviors of a boost converter operating with a state feedback control and with a constant power load while in reference [10], the authors studied a buck converter in a closed loop.

Some studies involved, for example, Sliding Mode Control [23], Fuzzy Logic [24], [25], Non-linear Proportional Integral [26], as well as many others linear and non-linear [27], [28].

Let us also mention feedback linearization [29], synergetic control [30], pulse adjustment technique [31], or active damping. Active damping was primarily used to stabilize the input filter of AC/DC converters [32], [33] as well as the output filter of power-electronic inverters [34].

In reference [30], the authors stabilize a buck converter loaded with a non-ideal constant power load using a Synergetic control while reference [35] consists in a study of a synchronous generator-rectifier which feeds a constant power load.

Reference [34] shows a new way of dealing with the negative impedance issue which is called Pulse Adjustment. In a few words, it is a frequency digital control technique where the converters are treated as digital systems and where the output voltage regulation is achieved by choosing high and low power pulses instead of the conventional pulse width modulation.

Let us also highlight references [36], [37], where the authors deal with various methods to overcome the destabilizing problem of the negative impedance. A stability analysis of an open loop converter is performed in [38], [39] and [40].

In reference [41], the authors are using a Nonlinear System Stability Controller (NSSC) based on a stability criterion that predicts when the overall system is unstable. This criterion also allows the use of several other methods to stabilize the system. Let us mention the design of the converter regulatory control with low bandwidth which reduces the negative impedance or this other method which consists in incorporating a passive RC damping network.

Reference [42] shows another method which consists in the use of a linear feed forward pole-zero cancellation control.

Reference [43] shows a study of a converter loaded by a constant power load and operating in Discontinuous Conduction Mode (DCM). They prove that the system is stable when

running in open loop. Besides, the authors also show that the feedback design of a DC/DC converter loaded by a constant power load can be designed as a conventional feedback with a resistive load.

The authors of reference [44] explain how to stabilize a microgrid loaded with a constant power load using amplitude death. They focus on two methods to provide an open loop control: one using delay, the other using circuit heterogeneity.

Reference [45] exhibits a virtual resistance method based on active damping to stabilize a microgrid.

In reference [46], the authors studied a matrix converter feeding a three-phase constant power load. They averaged the model using the state average method.

In reference [47], the author divided the different methods to compensate the constant power load into three categories which consist in:

- making the feeder more robust
- inserting a element between the feeder and the load
- doing some modifications in the load itself

Figure [11] represents a summary of all those methods.

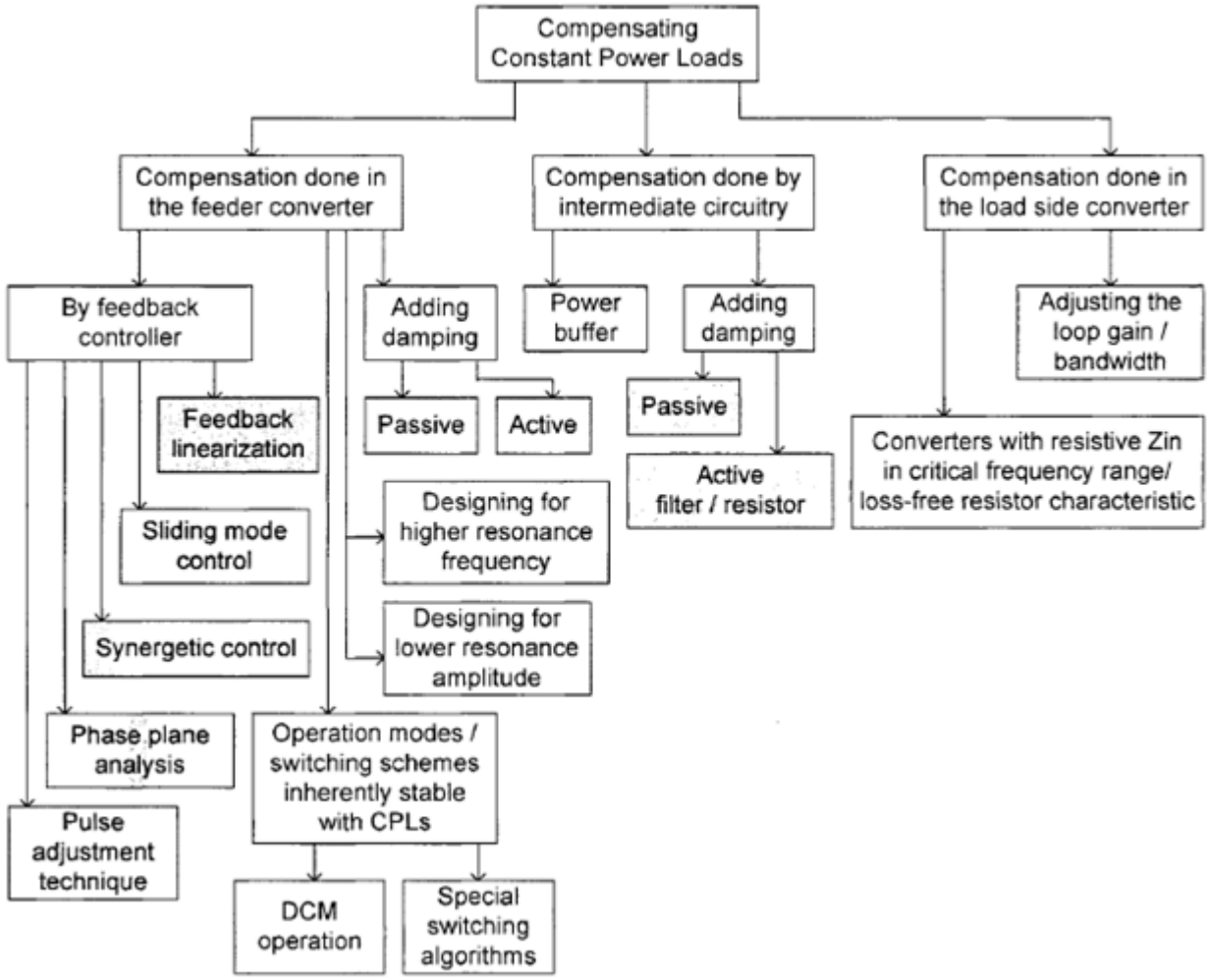

Figure 11: Summary of the different methods used to compensate the negative effect of a constant power load

3.0 DESCRIPTION OF THE SYSTEM

3.1 MODEL

As it has been seen in the literature review, the negative impedance of the constant power load is a recurrent issue in power electronics. Whenever a constant power load is used, an instability problem might be encountered. Let us consider our model, shown in figure [12].

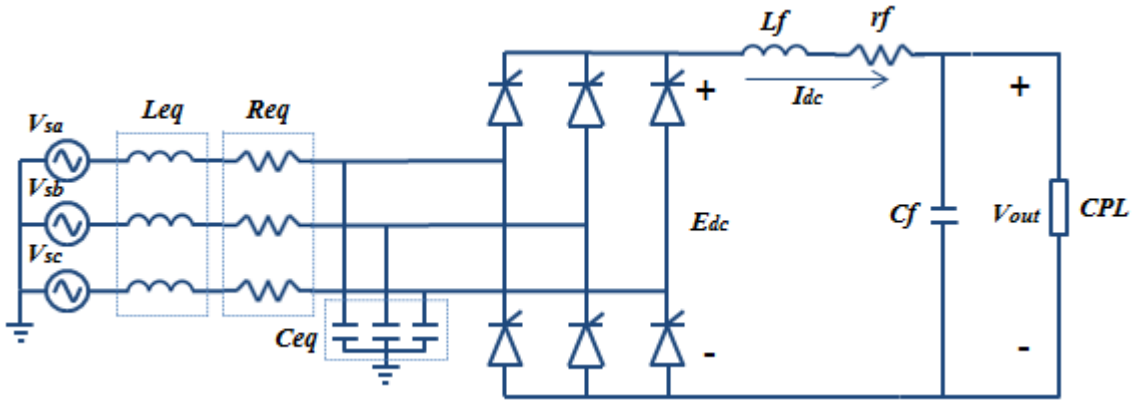

Figure 12: Three-phase rectifier feeding a constant power load

This circuit is quite simple, it consists of:

- a balanced three-phrase voltage source: V_{sa}, V_{sb} and V_{sc}
- a transmission line: R_{eq}, L_{eq} and C_{eq}
- a 6-pulse controlled rectifier
- filters: r_f, L_f and C_f
- a constant power load

In this case, the constant power load is a mathematical model. In real application, the constant power load could be a boost converter for example.

A similar study on this converter has already been done in reference [48]. The authors studied the stability problems and limits. However, this study can significantly be improved. It has already been improved in reference [49] where the authors used Artificial Intelligence techniques to enhance the control of the system. These two techniques were Adaptive Tabu Search and Genetic Algorithm.

This being so, this system can be improved using an optimal control method. Then it will be possible to reach a new threshold regarding the stability limits.

Figure [13] shows how the control strategy is applied on the system.

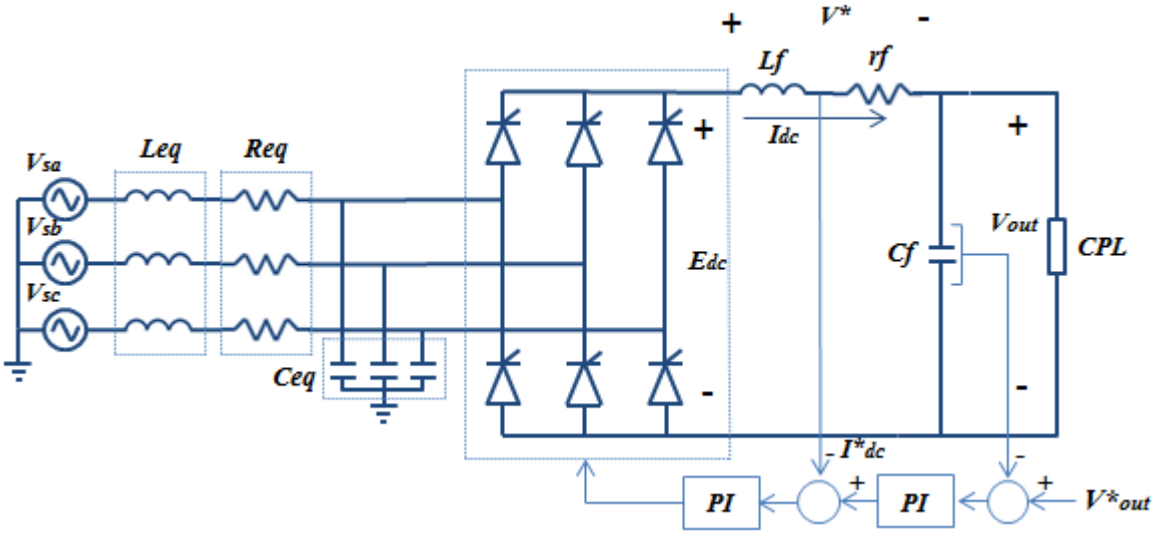

Figure 13: Model including the control system

3.2 CONTROL STRATEGY

This control strategy is made by the use of two PI controllers. Because the model a mathematical model, it is necessary to simulate a constant power load. To to that, one PI controller will control the output voltage while the second PI controller will maintain the current constant on the DC side.

Figure [14] represents the schematic of the two PI controllers.

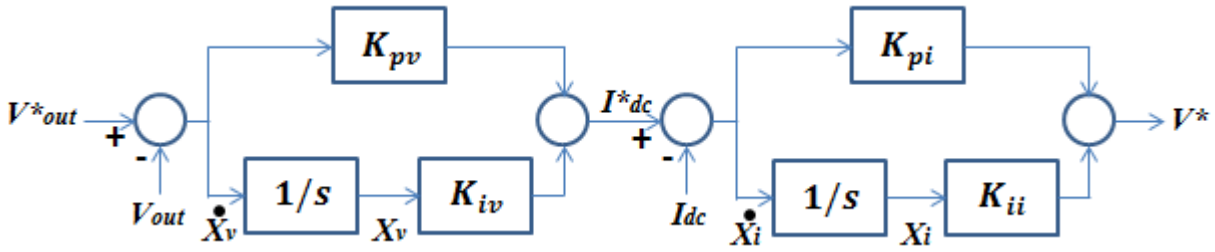

Figure 14: Schematic of the controllers

Basically, the goal is to control the voltage V^*, which is the voltage accross the two DC side components: r_f and L_f, through the use of the two PI controllers.

In the two studies mentioned above, the control scheme was the same. Consequently, in both studies, they managed to find some values for the four coefficients of the two PI controllers: K_{pv}, K_{iv}, K_{pi} and K_{ii}. In reference [48], the authors used a classical method to determine the four coefficients of the two PI controllers. On the other hand, in reference [49], they used the Adaptive Tabu Search and the Genetic Algorithm to determine the four parameters.

Let us give more information about these two PI controllers. Each one controls one loop:

- a current control loop
- a voltage control loop

The two controllers are built according to figure [15] and figure [16]. Figure [15] represents the current control loop.

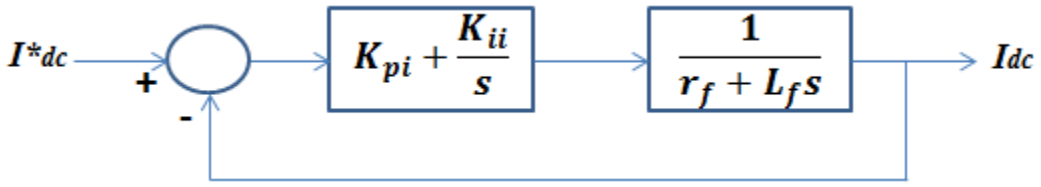

Figure 15: Current control loop

The components of this control block diagram are:

- the reference signal: I^*_{dc}
- the output signal: I_{dc}
- the controller with the two coefficients:
  - proportional gain: K_{pi}
  - integral gain: K_{ii}
- the plant with the two components to regulate:
  - the resistance r_f
  - the inductance L_f

Let us focus on the voltage control loop, represented in figure [16].

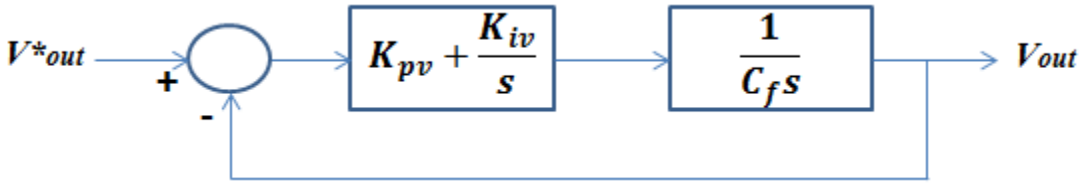

Figure 16: Voltage control loop

The components of this control block diagram are:

- the reference signal: V_{out}^{*}
- the output signal: V_{out}
- the controller with the two coefficients:
  - proportional gain: K_{pv}
  - integral gain: K_{iv}
- the plant with the component to regulate:
  - the capacitance C_f

The current control loop is the inner loop, while the voltage control loop is the outer loop. The four coefficients will be calculated in the next chapter using the Classical Method.

4.0 DEVELOPMENT OF THE SOLUTION

4.1 TRANSFORMATION METHODS

As shown in the previous part, the model is represented in figure [13].

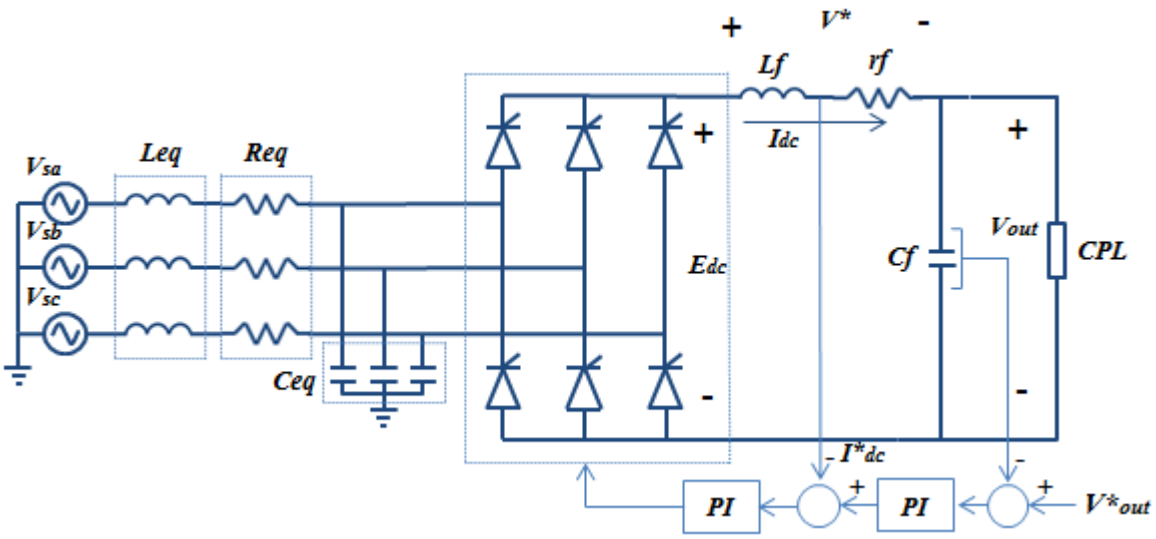

This circuit has to be derived in order to be transformed in matrix form. Once it will be mathematically modeled, it will be possible to apply the new control strategy through the use of MATLAB.

Besides, it is necessary to derive this circuit since this model is time-varying. In fact, the system is time-varying because of the switching behaviors of the converter. Hence, the system is more complicated to study. These switching behaviors have to be eliminated in order to obtain a time-invariant system. A time-invariant model is easier to deal with and makes possible to apply the classical linear system theory on it.

To derive a circuit like this, there are several methods:

- State-Space Averaging
- Average-Value Modeling
- dq-transformation

For each method, there are some advantages. For example, the State-Space Averaging offers [50]:

- A more compact representation of equations.
- A comfort to obtain both DC and AC transfer functions.

The Average-Value method offers a very good accuracy for modeling but is not easily applicable.

However, the most used is the dq-transformation method which is also the most convenient and most useful one. Let us give more information about the dq-transformation method [51]. This method consists in a transformation of coordinates. It transforms the three-phase stationary system into the dq rotating system. Two distinct steps are needed to perform this transformation:

- First step

  Transformation from the three-phase stationary coordinate scheme into the two-phase stationary coordinate scheme. The two-phase stationary coordinate system is usually named the $\alpha\beta$ system.

- Second step

  Transformation from the two-phase stationary coordinate system into the dq rotating coordinate system.

Let us consider a three-phase balanced system, it is possible to transform it into the dq system through the use of matrix T shown in equation (4.1).

$$T = \frac{2}{3}\begin{bmatrix} cos(\omega t) & cos(\omega t - \frac{2}{3}\pi) & cos(\omega t + \frac{2}{3}\pi) \\ -sin(\omega t) & -sin(\omega t - \frac{2}{3}\pi) & -sin(\omega t + \frac{2}{3}\pi) \end{bmatrix} \tag{4.1}$$

In other words, it is possible to obtain the transformation of a matrix X_{abc}, shown in equation (4.2), to a matrix X_{dq}, shown in equation (4.3).

$$X_{abc} = \begin{bmatrix} X_a \\ X_b \\ X_c \end{bmatrix} \tag{4.2}$$

$$X_{dq} = \begin{bmatrix} X_d \\ X_q \end{bmatrix} \tag{4.3}$$

This is summarized in equation (4.4).

$$X_{dq} = T \times X_{abc} \tag{4.4}$$

It is also possible to transform X_{dq} into X_{abc} via the multiplication of T^{-1}.

The dq-transformation is the method used in this study.

Figure [17] represents the application of the dq-transformation to the stator of a synchronous machine. The left hand side shows the three-phase stationary coordinate system, while the right hand side highlights the dq rotating coordinate system [1].

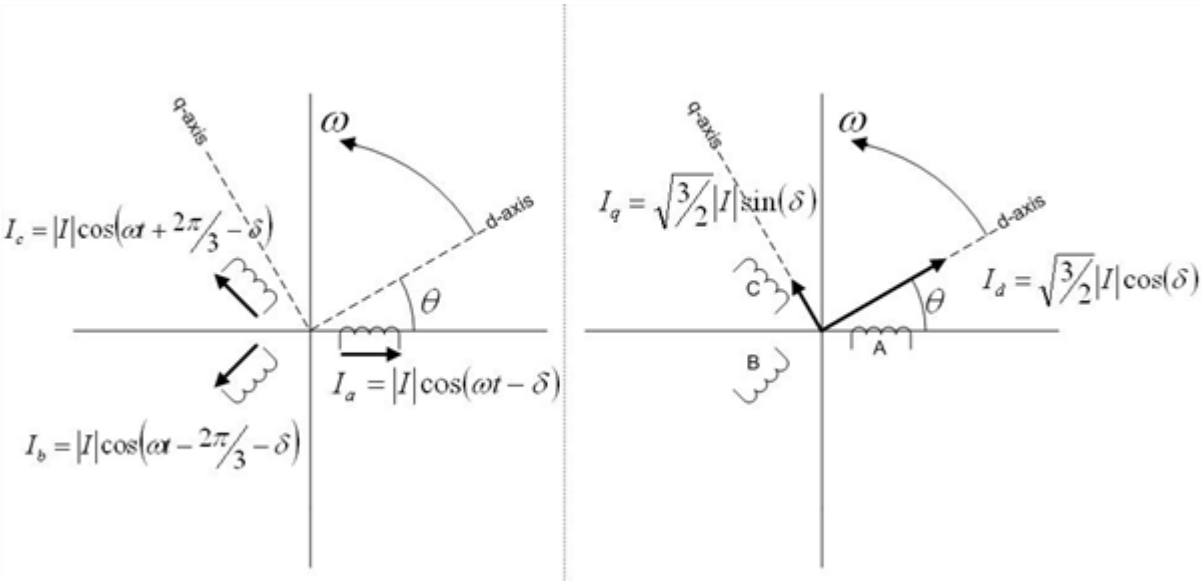

Figure 17: dq-transformation - Adapted from Reference [1]

One last interesting point about the dq-transformation is that the power converters can be treated as power transformers.

4.2 DQ-TRANSFORMATION OF THE MODEL

This dq-transformation is divided into three parts. First, let us transform only the rectifier into the dq form. Second, the different components present in the original circuit will be added. And finally, the model of the second step will be simplified [52].

Before doing the transformation, it is important to mention the following assumptions:

- The converter is operating under the continuous conduction mode.
- A constant output current of the rectifier is assumed.
- The amplitudes of the three-phase sources are constant and balanced.
- Harmonics are neglected.
- The overlap angle resistance caused by the effect of L_{eq} on the AC side is also neglected.

As a reminder, figure [12] represents the original model without the controllers.

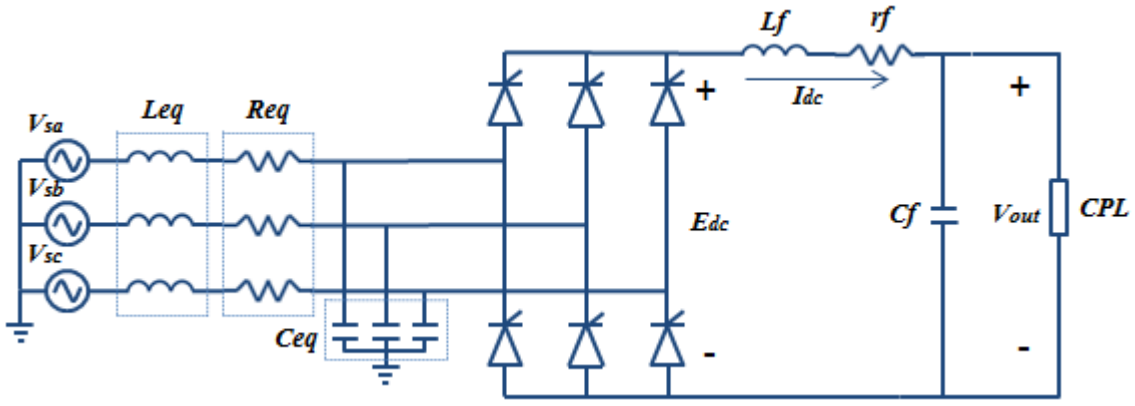

The controls applied to the circuit are not included in the dq-transformation.

Let us begin by deriving the switching signals of the controlled rectifier, represented in figure [18] and express them in Fourier series, as shown in equation (4.5). Let us remind that the harmonics are neglected.

$$S_{abc} = \frac{2\sqrt{3}}{\pi}\left[sin(\omega t + \phi - \alpha) \quad sin(\omega t - \tfrac{2}{3}\pi + \phi - \alpha) \quad sin(\omega t + \tfrac{2}{3}\pi + \phi - \alpha)\right]^T \tag{4.5}$$

Where ϕ is the phase angle of the AC bus and α is the firing angle of the thyristors.

Equations (4.6) and (4.7) represent the transfer functions of the controlled rectifier:

$$I_{in,abc} = S_{abc} I_{dc} \tag{4.6}$$

$$E_{dc} = S_{abc}^T V_{bus,abc} \tag{4.7}$$

Let us now apply matrix T on equations (4.6) and (4.7) which become equations (4.8) and (4.9).

$$I_{in,dq} = S_{dq} I_{dc} \tag{4.8}$$

$$E_{dc} = S_{dq}^{T} V_{bus,dq} \tag{4.9}$$

Equation (4.10) is the transformation of equation (4.5).

$$S_{dq} = \sqrt{\frac{3}{2}} \frac{2\sqrt{3}}{\pi} \begin{bmatrix} cos(\phi_1 - \phi + \alpha) & -sin(\phi_1 - \phi + \alpha) \end{bmatrix}^T \tag{4.10}$$

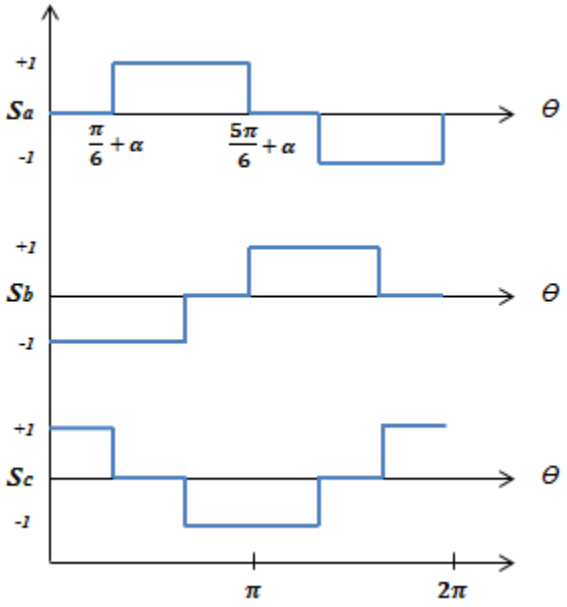

Figure 18: Switching functions

With equations (4.8), (4.9) and (4.10), it is possible to draw the dq representation of the controlled rectifier. It is represented as two power transformers. One depends on d and has a ratio S_d while the second one depends on q and then has a ratio S_q.

Those ratios depend on:

- the phase of the dq frame ϕ_1
- the phase of the AC bus ϕ
- the firing angle α

Figure [19] is the dq representation of the rectifier only.

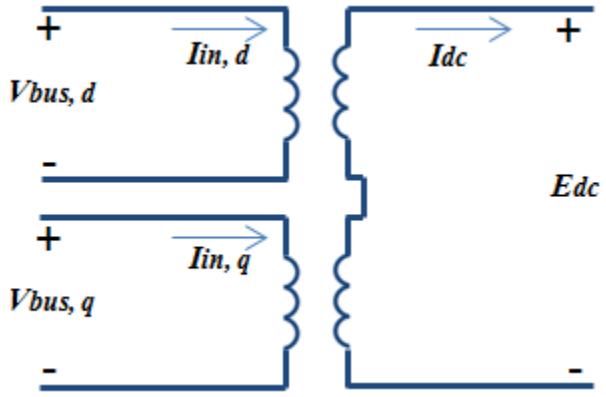

Figure 19: dq representation of the rectifier

The input, which was a three-phase, has been replaced by two inputs. The rectifier is now in dq form, so the rest of the circuit must be transformed too via the use of matrix T. Figure [20] represents the rectifier modeled in figure [19] plus the different components present in the original circuit.

In a few words, the transmission lines have been transformed in dq form: the components R_{eq} and L_{eq} have added a voltage source in series while the capacitance C_f has added a current source in parallel [53].

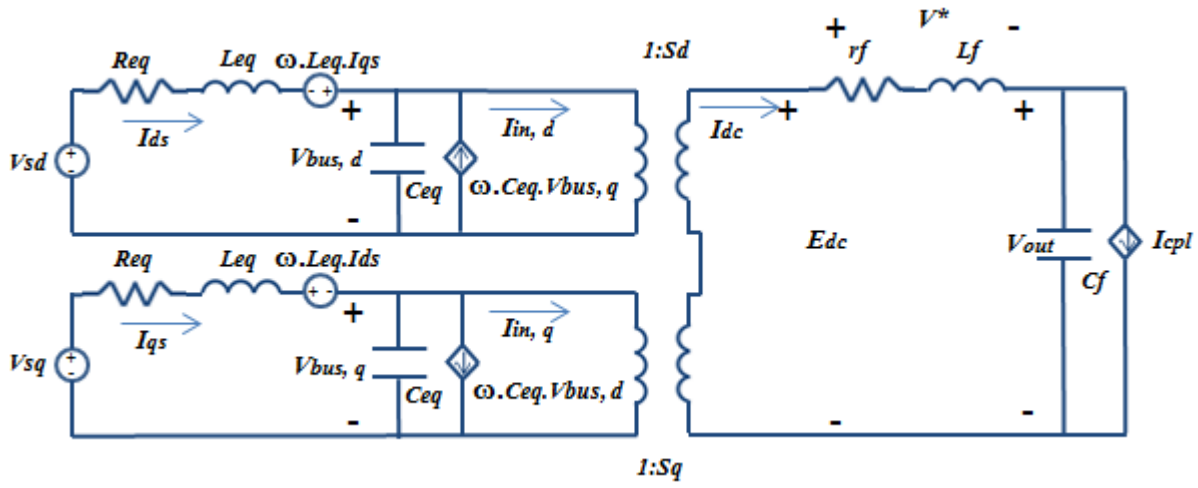

Figure 20: dq representation of the whole circuit

The three-phase sources V_{sa}, V_{sb} and V_{sc} have been eliminated and replaced by the dq sources V_{sd} and V_{sq}.

The last step is to simplify the complete model by fixing the rotating frame on the phase of the switching function, represented in equation (4.11).

$$\phi_1 = \phi - \alpha \tag{4.11}$$

By considering equation (4.11), the q term of equation (4.10) will be canceled. Consequently, the ratio $1 : S_q$ of the second transformer will be equal to $1 : 0$ and so this part of the circuit can be neglected.

The simplified model is shown in figure [21].

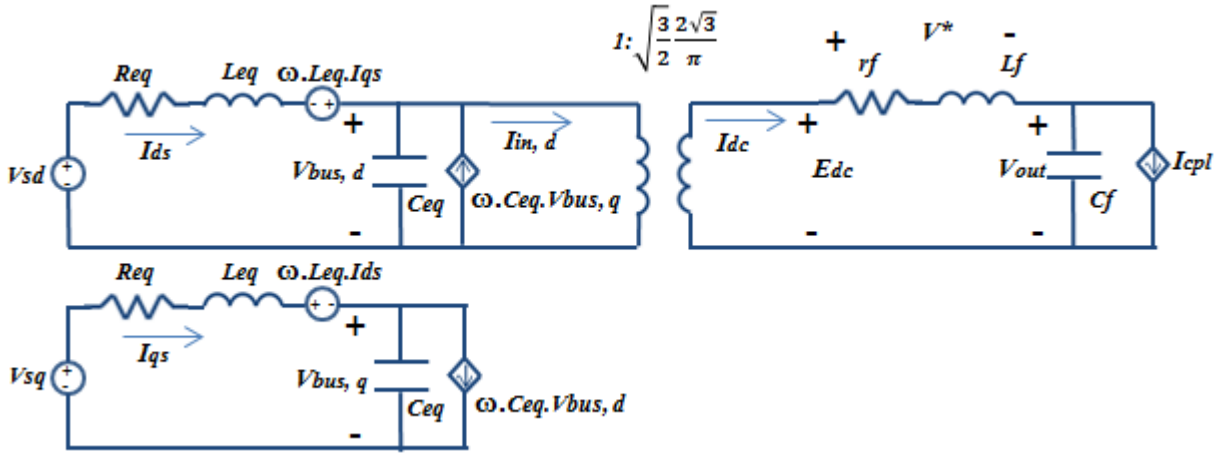

Figure 21: Simplified model of dq-transformation

4.3 DERIVATION OF THE CONTROLLERS' EQUATIONS

Let us now consider the controls associated with the system because so far the circuit has been transformed in the dq form without taking the controllers into account. Let us remind the control schematic with the two PI controllers in figure [14].

Let us first derive V^* according to the schematic of the controllers, represented in equation (4.12).

$$V^* = -K_{pi}I_{dc} - K_{pv}K_{pi}V_{out} + K_{iv}K_{pi}X_v + K_{ii}X_i + K_{pv}K_{pi}V^*_{out} \tag{4.12}$$

Then let us give the differential equation for X_v and X_i, shown in equation (4.13) and (4.14).

$$\dot{X}_v = -V_{out} + V^*_{out} \tag{4.13}$$

$$\dot{X}_i = -I_{dc} - K_{pv}V_{out} + K_{iv}X_v + K_{pv}V^*_{out} \tag{4.14}$$

Besides, it has been mentioned earlier in this study that the voltage V^* is controlled via the resistance r_f and the inductance L_f. This is shown in equation (4.15).

$$V^* = r_f I_{dc} + L_f \dot{I}_{dc} \tag{4.15}$$

The equation of $\dot{I}_{dc}$ is obtained in equation (4.16) after substituting equation (4.12) into (4.15).

$$\dot{I}_{dc} = -\frac{r_f + K_{pi}}{L_f} I_{dc} + \frac{K_{iv} K_{pi}}{L_f} X_v + \frac{K_{ii}}{L_f} X_i - \frac{K_{pv} K_{pi}}{L_f} V_{out} + \frac{K_{pv} K_{pi}}{L_f} V^*_{out} \tag{4.16}$$

The set of equations for the controllers schematic has been obtained. Let us now derive in the following section the equations of figure [21].

4.4 DERIVATION OF THE DQ SIMPLIFIED MODEL'S EQUATIONS

To derive the simplified model's equations, let us use the well-known Kirchhoff's voltage and current laws. By applying Kirchhoff's laws, the following set of non-linear equations has been obtained. This set of equations is represented in equation (4.17) to equation (4.21).

$$\dot{I}_{ds} = -\frac{R_{eq}}{L_{eq}} I_{ds} + \omega I_{qs} - \frac{1}{L_{eq}} V_{bus,d} + \frac{1}{L_{eq}} V_{sd} \tag{4.17}$$

$$\dot{I}_{qs} = -\frac{R_{eq}}{L_{eq}} I_{qs} - \omega I_{ds} - \frac{1}{L_{eq}} V_{bus,q} + \frac{1}{L_{eq}} V_{sq} \tag{4.18}$$

$$\dot{V}_{bus,d} = \frac{1}{C_{eq}} I_{ds} + \omega V_{bus,q} - \sqrt{\frac{3}{2}} \frac{2\sqrt{3}}{\pi C_{eq}} I_{dc} \tag{4.19}$$

$$\dot{V}_{bus,q} = -\omega V_{bus,d} + \frac{1}{C_{eq}} I_{qs} \tag{4.20}$$

$$\dot{V}_{out} = \frac{1}{C_f} I_{dc} + \frac{1}{C_f} \frac{P_{cpl}}{V_{out}} \tag{4.21}$$

Now that all the necessary equations have been derived, the next step is to linearize them in order to be put in matrix form.

4.5 LINEARIZATION

The set of equation must be linearized around the operating point V_{out}^{*}. Then, a set of linear differential equations will be obtained and put in matrix form, according to the well-known state-space form shown in equation (4.22).

$$\begin{aligned} \partial\dot{x} &= A(x_0, u_0)\partial x + B(x_0, u_0)\partial u \\ \partial y &= C(x_0, u_0)\partial x + D(x_0, u_0)\partial u \end{aligned} \tag{4.22}$$

Then matrix A is created and given in equation (4.23).

$$A(x_0, u_0) = \begin{bmatrix} -\frac{R_{eq}}{L_{eq}} & \omega & -\frac{1}{L_{eq}} & 0 & 0 & 0 & 0 & 0 \\ -\omega & -\frac{R_{eq}}{L_{eq}} & 0 & -\frac{1}{L_{eq}} & 0 & 0 & 0 & 0 \\ \frac{1}{C_{eq}} & 0 & 0 & \omega & -\sqrt{\frac{3}{2}}\frac{2\sqrt{3}}{\pi C_{eq}} I_{dc} & 0 & 0 & 0 \\ 0 & \frac{1}{C_{eq}} & -\omega & 0 & 0 & 0 & 0 & 0 \\ 0 & 0 & 0 & 0 & -\frac{r_f + K_{pi}}{L_f} & -\frac{K_{pv}K_{pi}}{L_f} & \frac{K_{iv}K_{pi}}{L_f} & \frac{K_{ii}}{L_f} \\ 0 & 0 & 0 & 0 & \frac{1}{C_f} & \frac{P_{cpl}}{C_f V_{out,0}^2} & 0 & 0 \\ 0 & 0 & 0 & 0 & 0 & -1 & 0 & 0 \\ 0 & 0 & 0 & 0 & -1 & -K_{pv} & K_{iv} & 0 \end{bmatrix} \tag{4.23}$$

Matrix A is a 8×8 matrix since there were 8 equations after the derivation of the simplified model. Matrix B is shown in equation (4.24).

$$B(x_0, u_0) = \begin{bmatrix} 0 \\ 0 \\ 0 \\ 0 \\ \frac{K_{pv} Kpi}{L_f} \\ 0 \\ 1 \\ K_{pv} \end{bmatrix} \tag{4.24}$$

Matrices C and D are represented in equations (4.25) and (4.26).

$$C(x_0, u_0) = \begin{bmatrix} 0 & 0 & 0 & 0 & 0 & 1 & 0 & 0 \end{bmatrix} \tag{4.25}$$

$$D(x_0, u_0) = \begin{bmatrix} 0 \end{bmatrix} \tag{4.26}$$

It is also important to show the matrices of the states X, the input U and the output Y. They are respectively given in equations (4.27), (4.28) and (4.29).

$$x = \begin{bmatrix} I_{ds} & I_{qs} & V_{bus,d} & V_{bus,q} & I_{dc} & V_{out} & X_v & X_i \end{bmatrix}^T \tag{4.27}$$

$$u = \begin{bmatrix} V_{out}^* \end{bmatrix} \tag{4.28}$$

$$y = \begin{bmatrix} V_{out} \end{bmatrix} \tag{4.29}$$

4.6 DETERMINATION OF THE CONTROLLERS' COEFFICIENTS

To simulate the model in MATLAB, it is necessary to give the value of the following parameters:

- $V_s = 230V_{rms}/phase$
- $f = 50Hz$
- $R_{eq} = 0.15\Omega$
- $L_{eq} = 30\mu H$
- $C_{eq} = 2nF$
- $C_f = 1000\mu F$
- $r_f = 0.03\Omega$
- $L_f = 6.5mH$

Let us now find the value of the four coefficients K_{pv}, K_{iv}, K_{pi} and K_{ii}. Let us remind Figure [15] which represents the current control loop and figure [16] which represents the voltage control loop.

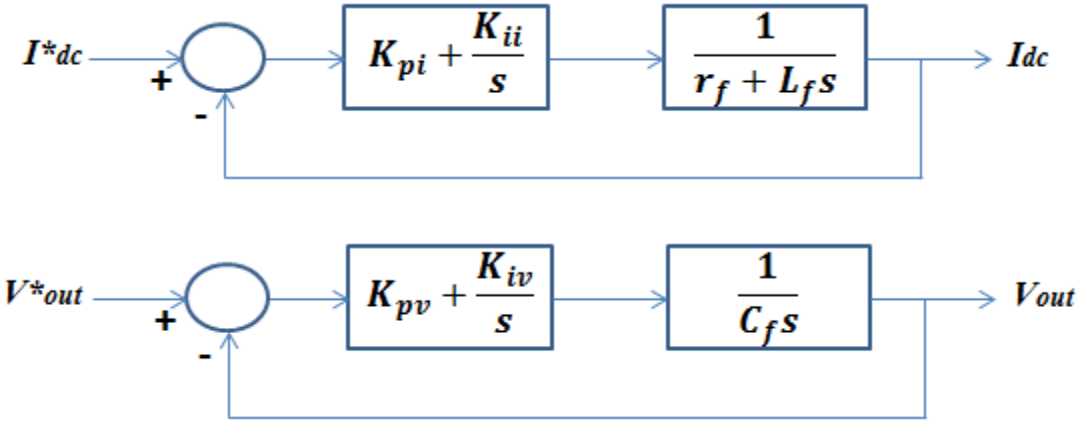

To find the values of these coefficients, let us use the Classical method. The first step is to find the transfer function of the current control loop. This is shown in equation (4.30).

$$\frac{I_{dc}}{I_{dc}^*} = \frac{sK_{pi} + K_{ii}}{s^2 + (\frac{K_{pi}+r_f}{L_f})s + \frac{K_{ii}}{L_f}} \tag{4.30}$$

Previously, some values for the DC side parameters L_f and r_f have been given. These values will be necessary to determine the parameters values of the two PI controllers. To

determine the parameters K_{pi} and K_{ii}, let us use the denominator of the canonical form of a second order system shown in equation (4.31).

$$s^2 + 2\xi\omega_n s + \omega_n^2 \tag{4.31}$$

Next step is to identify the different components knowing that the values of the damping ration ξ and the natural frequency ω_{ni} are respectively 0.8 and $2\pi 70 rad/s$. By identification, let us find the equations for K_{pi} and K_{ii}. Those are shown in equations (4.32) and (4.33).

$$K_{pi} = 2\xi\omega_{ni}L_f - r_f \tag{4.32}$$

$$K_{ii} = \omega_{ni}^2 L_f \tag{4.33}$$

After doing the calculation, the values of K_{pi} and K_{ii} are respectively 4.5442 and 1257.4.

Let us now do the same analysis for K_{pv} and K_{iv} which are the parameters of the voltage control loop. By considering figure [16], let us write the transfer function of the voltage control loop, as shown in equation (4.34).

$$\frac{V_{out}}{V_{out}^*} = \frac{sK_{pv} + K_{iv}}{s^2 + (\frac{K_{pv}}{C_f})s + \frac{K_{iv}}{C_f}} \tag{4.34}$$

In this case, only the value of the capacitance C_f is required to determine the coefficients K_{pv} and K_{iv} of the PI controller. Again, let us compare and identify K_{pv} and K_{iv} with the denominator of the canonical form of a second order system and using a damping ratio $\xi = 0.8$ and a natural frequency $\omega_{nv} = 2\pi 10 rad/s$, as shown in equations (4.35) and (4.36).

$$K_{pv} = 2\xi\omega_{nv}C_f \tag{4.35}$$

$$K_{iv} = \omega_{nv}^2 C_f \tag{4.36}$$

After doing the calculation, the values of K_{pv} and K_{iv} are respectively 0.101 and 3.9478.

4.7 LINEAR QUADRATIC REGULATOR

The Linear Quadratic Regulator method is a well-known optimal control method. MATLAB offers a useful toolbox to apply this method. Basically, the Linear Quadratic Regulator function on MATLAB will select the optimal coefficients K to stabilize the system. The purpose is to minimize the quadratic cost function given in equation (4.37) by using the state feedback law shown in equation (4.38) [54]. This optimal control method implies having a full knowledge of the states: full state feedback.

$$J(u) = \int_0^\infty (x^T Q x + u^T R u + 2x^T N u)\,\mathrm{d}t \tag{4.37}$$

$$u = -KX \tag{4.38}$$

In order to obtain a usable answer for the step input, it is necessary to add a feed forward gain K_f to compensate and obtain a DC gain equal to unity. This gain is calculated in equation (4.43).

$$K_f = \frac{1}{C(-A + BK)^{-1}B} \tag{4.39}$$

Let us remind that in this study, V_{out}^* is the input. The system of equation (4.39) represents the standart state-space form without matrix D which is equal to zero.

$$\begin{aligned} \dot{X} &= AX + Bu \\ Y &= CX \end{aligned} \tag{4.40}$$

Let us now subsitute equation (4.40), which is coming from figure [22] into (4.39) to obtain equation (4.41)

$$u = V_{out}^* K_f - KX \tag{4.41}$$

$$\begin{aligned} \dot{X} &= AX + B(V_{out}^* K_f - KX) \\ Y &= CX \end{aligned} \tag{4.42}$$

Equation (4.42) is obtained from equation (4.41) after being rearranged.

$$\begin{aligned} \dot{X} &= (A - BK)X + BV^*_{out}K_f \\ Y &= CX \end{aligned} \tag{4.43}$$

Figure [22] represents the schematic of the solution. The plant is considered to be the whole system.

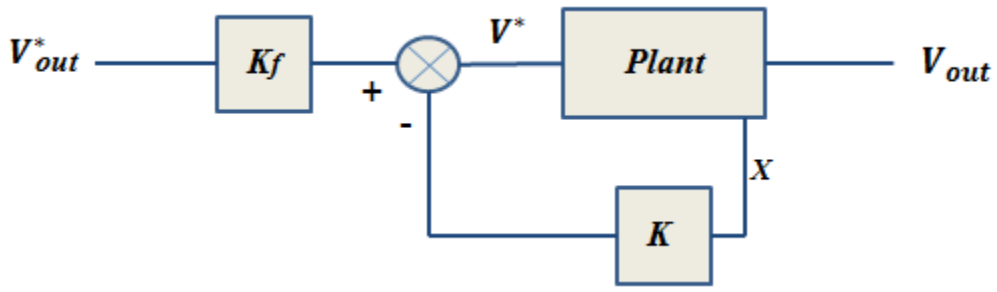

Figure 22: Schematic of the new control strategy

Now that everything is set, let us implement the derived system in MATLAB.

5.0 SIMULATIONS AND RESULTS

5.1 RESULTS FOR THE ORIGINAL CONTROL STRATEGY

As we mentioned previously, the goal of the study is to enhance the stability of the given circuit. The original control scheme is able to give good results and it will not be modified. However, it is possible to improve the system's stability using the optimal control method.

In order to do this, let us apply the Linear Quadratic Method studied in the previous chapter. Applying this method on the whole system will greatly enhance the system's stability.

In this chapter, the system's stability will be analysed, but the system's behaviors will also be studied while the different parameters of the DC filter L_f and C_f will be changed. The goal is to observe what parameters have the potential to affect the stability of the system.

Before beginning the analysis, it is important to give the values for the different parameters which have not been given yet. Let us sort the parameters depending on the fixed or changing value.

Parameters with a fixed value:

- $V_s = 230V$
- $V_{out} = 500V$
- $f = 50Hz$
- $\omega = 2\pi f = 314rad/s$
- $R_{eq} = 0.15\Omega$
- $L_{eq} = 0.00003H$

- $C_{eq} = 0.000000002F$
- $r_f = 0.03\Omega$
- $K_{pv} = 0.10$
- $K_{iv} = 3.9478$
- $K_{pi} = 4.5442$
- $K_{ii} = 1257.4$

Parameters with a changing value:

- $C_f = 0.001F$
- $L_f = 0.0065H$
- $P_{cpl} = 25000W$

All the simulations show how the system reacts after being excited by a step. The first simulation is the most basic one. Only the two PI controllers are acting on the system with the values given previously. The result is shown in figure [23].

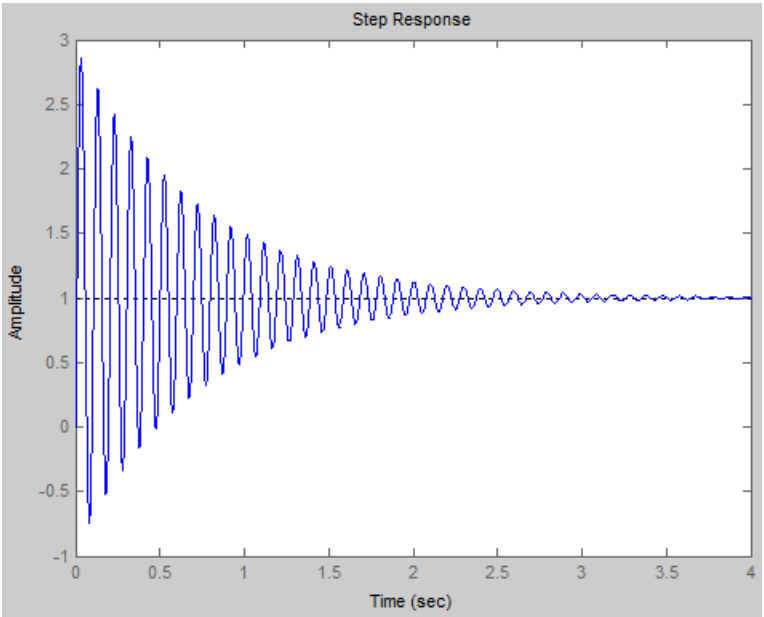

Figure 23: Original control strategy - Power = $25kW$

The power of the constant power load has been set to this value for a particular reason. Actually, $25kW$ represents the stability limit of the system. As it can be seen on figure [24], the system becomes unstable if the power has a value larger than $25.7kW$. To be precise, figure [24] represents the response of the system for a power equal to $26kW$.

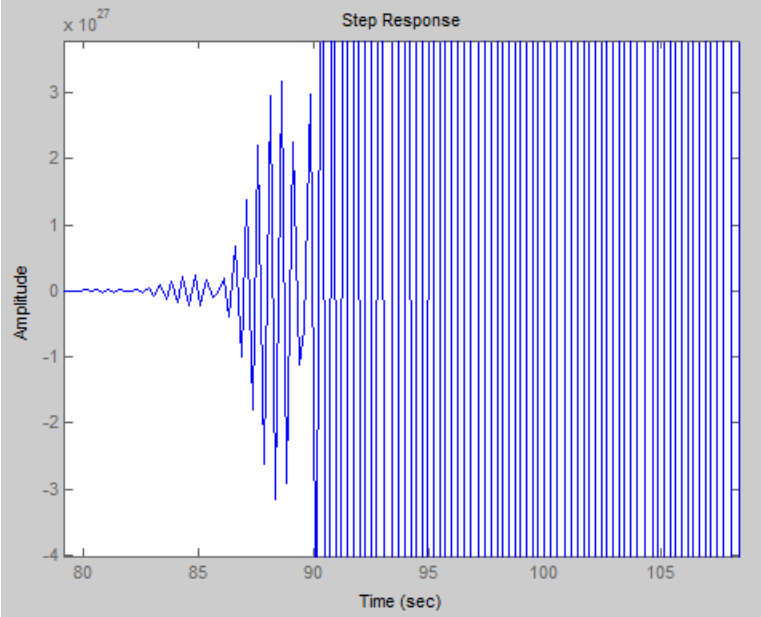

Figure 24: Original control strategy - Power = $26kW$

Another method used to check the stability is the Eigenvalue theorem. It requires less coding but on the other hand it is also less accurate and less convenient. Consider the two cases studied previously ($P_{cpl} = 25kW$ and $P_{cpl} = 26kW$).

In order to be stable, all the real parts of the eigenvalues of matrix A have to be less than 0 as shown in equation (5.1).

$$Re(\lambda i) < 0 \tag{5.1}$$

The eigenvalues can be calculated for matrix A using equation (5.2).

$$det(\lambda I - A) = 0 \tag{5.2}$$

The following set of eigenvalues is given in equation (5.3) and is simulated for a power of $25kW$.

$$\begin{aligned}
&-2499,99999999981 + 4082796,29843838i \\
&-2499,99999999981 - 4082796,29843838i \\
&-2499,99999999979 + 4082167,97990765i \\
&-2499,99999999979 - 4082167,97990765i \\
&-300,500190972646 + 312,545241021360i \\
&-300,500190972646 - 312,545241021360i \\
&-1,36134748889177 + 63,7231247560282i \\
&-1,36134748889177 - 63,7231247560282i
\end{aligned} \tag{5.3}$$

By simply looking at the real parts of the eigenvalue, it can be said that the system is stable since they are all less than 0. Now let us simulate the system again considering a power of $26kW$ for the constant power load. This new set of eigenvalues is given in equation (5.4).

$$\begin{aligned}
&-2499,99999999981 + 4082796,29843838i \\
&-2499,99999999981 - 4082796,29843838i \\
&-2499,99999999979 + 4082167,97990765i \\
&-2499,99999999979 - 4082167,97990765i \\
&-300,572562113903 + 311,945780393577i \\
&-300,572562113903 - 311,945780393577i \\
&0,711023652364315 + 63,7898661009897i \\
&0,711023652364315 - 63,7898661009897i
\end{aligned} \tag{5.4}$$

In this case, it can be noticed that the two last eigenvalues have a positive real part. It confirms figure [24] which shows that the system becomes unstable.

As mentioned, another goal of the study is to analyze the behaviors of the stability limits considering a change in the DC filters' parameters. Figure [25] shows how the limits react with a change in the capacitance C_f.

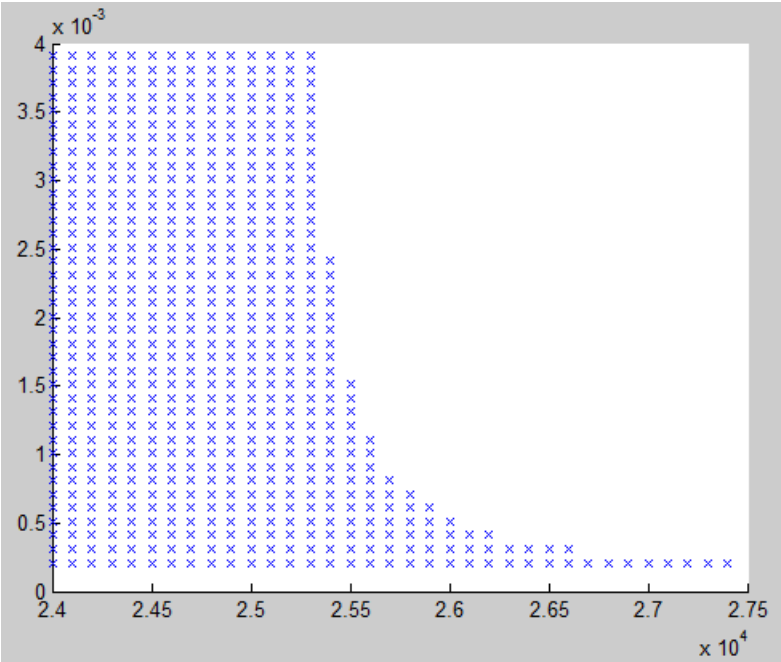

Figure 25: Original control strategy - for a varying C_f

Basically, it can be observed that the capacitance C_f have an effect on the stability of the system. Different values for C_f (from $10\mu F$ to $4000\mu F$) have been tried for a varying power (from $24kW$ to $34kW$). It is possible to reach a stable region for some values of the C_f. For example, for 24 kW, the stable region can be reached for any value of C_f. Consider now a power of $27kW$, the stable region can be reached for a capacitance C_f equal to $210\mu F$.

Let us do the same analysis for the inductance L_f. Figure [26] is representing the results.

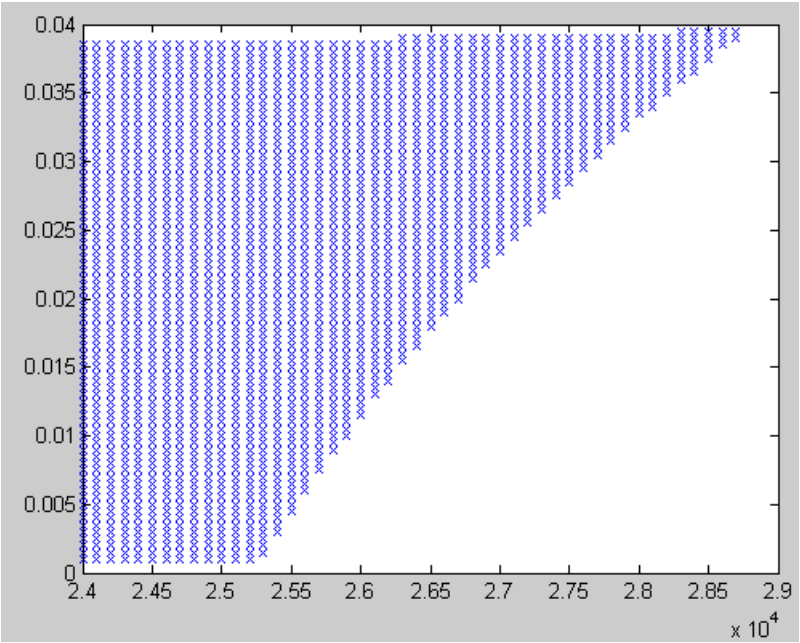

Figure 26: Original control strategy - for a varying L_f

As it can be seen in figure [26], the inductance L_f has a different effect than the capacitance C_f on the stability limits. The range for L_f is very large: it is varying from $0H$ to $0.05H$ for the same range of power as the previous analysis (from $24kW$ to $35kW$). The original value of L_f was $0.0065H$. The close variation around this point does not affect the stability. However, a stable region can be reached with a higher power ($29kW$) using a larger value of L_f. It has to be mentioned that we reach the stability limit for which L_f can no longer help at $29kW$.

5.2 RESULTS AFTER APPLYING THE LINEAR QUADRATIC REGULATOR METHOD

Let us now apply the Linear Quadratic Regulator method on the whole system.

Figure [27] shows how the system reacts when excited by a step after applying the control method.

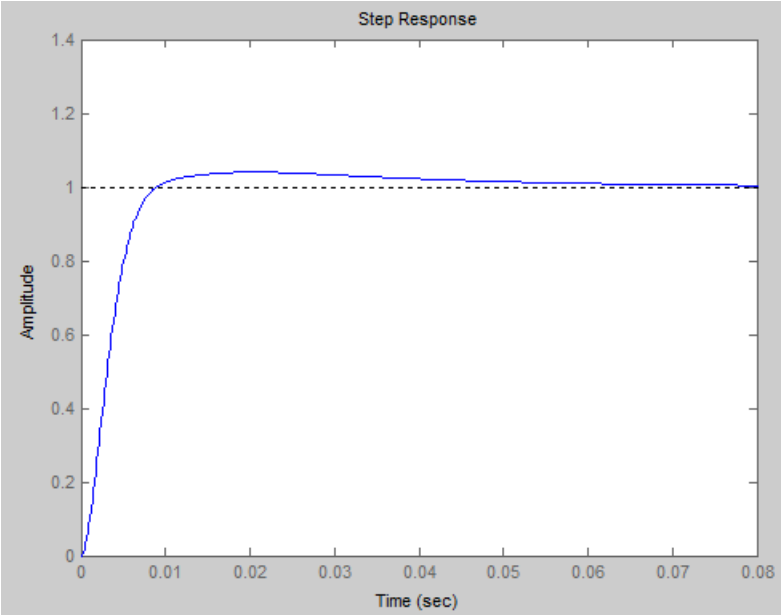

Figure 27: New control strategy - Power = $25kW$

It is clear that the stability has tremendously been enhanced. By comparing with figure [23], the overshoot and the multiple oscillations have been eliminated. The new system is also faster. Besides, in figure [23] the stability was reached after 2.5 seconds while in figure [27], the stability is reached after 0.02 seconds. The behaviors of the system are now better.

Consider a power equal to $50kW$ for the constant power load, as simulated and shown in figure [28].

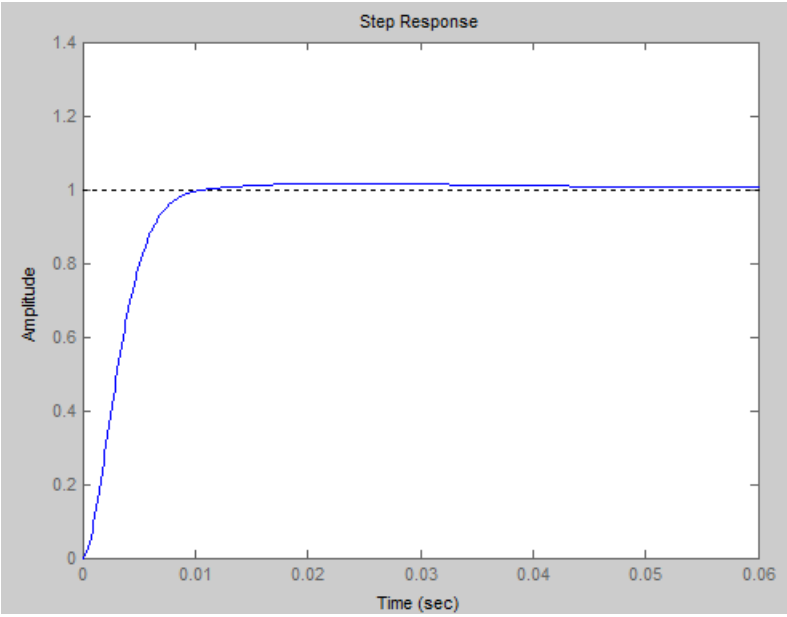

Figure 28: New control strategy - Power = $50kW$

The system is still stable, but with a less important overshoot.

In the original system, the stability limits have been determined. It has been noticed that for a power greater than approximately $26kW$, the system becomes unstable. However, in this case, the stability limit depends on the weight of the matrix Q that has been used to determine the optimal coefficients K. It has an influence on the general behavior of the system (overshoot, damping ratio, etc.). Matrix Q was chosen to be 1. However, it could have been a larger value. It totally depends on the applications requirements.

Let us mention that a larger value of Q, which means a larger control signal, will decrease the energy of the controller output. The inverse is also true: a smaller control signal will lead to an increase of the energy of the controller output [55]. Consequently, in theory it can be possible to find values for the weight of Q to stabilize the system. However, it may not be feasible in real application.

6.0 CONCLUSION

The study presented in the thesis focused on the improvement of the stability limits of a three-phase controlled rectifier feeding a constant power load.

The dq-transformation of the model was performed and validated throught simulations. The dq-transformation was used to derive the dynamic model of the system which was necessary to obtain a suitable model to be simulated. This model absolutely needed to be transformed to a time-invariant model.

Once the time-invariant model obtained, it was necessary to transform it in matrix form in order to be implemented in MATLAB. The different matrices were created according to the state-space form. To do so, the model was linearized around an operating point.

The Linear Quadratic Regulator method was applied on the original system which includes the two PI controllers used to maintain the system stable. The coefficients of the parameters of the two PI controllers were determined using the Classical control method. They were calculated according to specific values for the natural frequency of both loops and according to the damping ratio.

Originally, the system was stable until it reaches a power equal to $25kW$. It was possible to increase this limit by slightly changing the value of some parameters. By carefully choosing the value of the capacitance C_f, it was possible to increase the limit of power of $3kW$.

The Linear Quadratic Regulator method allowed the system to tremendously increase the limits of the stability. This method finds the values of the coefficients K to stabilize the system. The method will be always able to find values for K to keep the system stable, even for a large amount of power. However, this works in theory but it has some limits in real application. Indeed, it will not be possible to increase the power too much as the response of the system will not be able to satisfy the requirements. However, it should be

kept in mind that matrix Q of the Linear Quadratic Regulator method needs to be carefully parametered to fulfill the requirements of a real application. The larger the weight of matrix Q, the smaller the energy of the control output. The inverse is also true.

Finally, the goal of the thesis was reached; the stability of the system was considerably enhanced. However, the constant power load remains a problem, further investigation are necessary to find solutions which could work on most of the applications.

Besides, it would be interesting to repeat this study with a non-ideal constant power load to see how the system would react or directly use a boost converter instead of the mathematical model of the constant power load. Another idea for a future work would be to do the same analysis and include the harmonics.

BIBLIOGRAPHY

[1] "$http://en.wikipedia.org/wiki/dqo_transformation$."

[2] S. Roy, "Reliability considerations for data centers power architectures," *Telecommunications Energy Conference. INTELEC 2001. Twenty-Third International*, pp. 406–411, 2001.

[3] K. Mistry, E. Silverman, T. Taylor, and R. Willis, "Telecommunications power architectures: distributed or centralized." *Telecommunications Energy Conference. INTELEC 1989. Conference Proceedings., Eleventh International*, vol. 1, pp. 10.1/1–10.111, 1989.

[4] A. Kwasinski and P. Krein, "A microgrid-based telecom power system using modular multiple-input dc-dc converters," *Telecommunications Conference. INTELEC 2005. Twenty-Seventh International*, pp. 515–520, 2005.

[5] T. Gruzs and J. Hall, "Ac, dc or hybrid power solutions for today's telecommunications facilities," *Telecommunications Energy Conference. INTELEC 2000. Twenty-second International*, pp. 361–368, 2000.

[6] F. Bodi, "dc-grade reliability for ups in telecommunications data centers," *Telecommunications Energy Conference. INTELEC 2007. 29th International*, 2007.

[7] A. Monti, D. Boroyevich, D. Cartes, R. Dougal, H. Ginn, G. Monnat, S. Pekarek, F. Ponci, E. Santi, S. Sudhoff, N. Schulz, W. Shutt, and F. Wang, "Ship power system control: a technology assessment," *Electric Ship Technologies Symposium*, pp. 292–297, 2005.

[8] B. Johnson and R. Lasseter, "An industrial power distribution system featuring ups properties," *Power Electronics Specialists Conference*, vol. Power Electronics Specialists Conference. PESC 1993 Record., 24th Annual IEEE, pp. 759–765, 1993.

[9] W. Tang and R. Lasseter, "An lvdc industrial power distribution system without central control unit," *Power Electronics Specialists Conference. PESC 2000. 2000 IEEE 31st Annual*, vol. 2, pp. 979–984, 2000.

[10] M. Baran and N. Mahajan, "Dc distribution for industrial systems: opportunities and challenges," *IEEE Transactions on Industry Applications*, vol. 39, pp. 1596–1601, 2003.

[11] C. Rivetta and G. Williamson, "Large-signal analysis of a dc-dc buck power converter operating with constant power load," *Industrial Electronics Society. IECON 2003. The 29th Annual Conference of the IEEE*, vol. 1, pp. 732–737, 2003.

[12] A. Emadi, A. Khaligh, C. Rivetta, and G. Williamson, "Constant power loads and negative impedance instability in automotive systems: definition, modeling, stability, and control of power electronic converters and motor drives," *IEEE Transactions on Vehicular Technology*, vol. 55, pp. 1112–1125, 2006.

[13] C. Rivetta, G. Williamson, and A. Emadi, "Constant power loads and negative impedance instability in sea and undersea vehicles: Statement of the problem and comprehensive large-signal solution," *IEEE Electric Ship Technologies Symposium*, pp. 313–320, 2005.

[14] S. Danielsen, M. Molinas, T. Toftevaag, and O. B. Fosso, "Constant power load characteristic's influence on the low-frequency interaction between advanced electrical rail vehicle and railway traction power supply with rotary converters," *9th International Conference, Modern Electric Traction*, September 2009.

[15] S. Chirila, "Constant power load (kva) for ac load flow analysis," February 2002.

[16] L. Ying-xi, M. Xin-hua, G. Hong-juan, and J. Hua, "Stability study and simulation analysis on aircraft transformer rectifier unit (tru) with constant power load (cpl)," *Proceedings of the Eighth International Conference on Electrical Machines and Systems*, vol. 3, pp. 2018–2022, 2005.

[17] D. Ariyasinghe and D. Vilathgamuwa, "Stability analysis of microgrids with constant power loads," *IEEE International Conference on Sustainable Energy Technologies. ICSET 2008.*, pp. 279–284, 2008.

[18] A. Emadi, B. Fahimi, and M. Ehsani, "On the concept of negative impedance instability in advanced aircraft power systems with constant power loads," *34th Intersociety Energy Conversion Engineering Conference*, August 1999.

[19] A. Emadi and M. Ehsan, "Negative impedance stabilizing controls for pwm dc/dc converters using feedback linearization techniques," *Energy Conversion Engineering Conference and Exhibit, 2000. (IECEC) 35th Intersociety*, vol. 1, pp. 613–620, 2000.

[20] C. Rivetta and G. Williamson, "Global behaviour analysis of a dc-dc boost power converter operating with constant power load," *Circuits and Systems. ISCAS 2004. Proceedings of the 2004 International Symposium on*, vol. 5, pp. V–956–V–959, 2004.

[21] ——, "Large-signal analysis and control of buck converters loaded by dc-dc converters," *Power Electronics Specialists Conference. PESC 2004. IEEE 35th Annual*, vol. 5, pp. 3675–3680, June 2004.

[22] C. Rivetta, A. Emadi, G. Williamson, R. Jayabalan, and B. Fahimi, "Analysis and control of a buck dc-dc converter operating with constant power load in sea and undersea vehicles," *Industry Applications Conference, 2004. 39th IAS Annual Meeting. Conference Record of the 2004 IEEE*, vol. 2, pp. 1146–1153, 2004.

[23] H. Sira-Ramirez and M. Rios-Bolivar, "Sliding mode control of dc-to-dc power converters via extended linearization," *Fundamental Theory and Applications, IEEE Transactions on Circuits and Systems I*, vol. 41, pp. 652–661, 1994.

[24] S. Wing-Chi, C. Tse, and L. Yim-Shu, "Development of a fuzzy logic controller for dc/dc converters: design, computer simulation, and experimental evaluation," *IEEE Transactions on Power Electronics*, vol. 11, pp. 24–32, 1996.

[25] L. Bor-Ren and H. Chihchiang, "Buck/boost converter control with fuzzy logic approach," *Proceedings of the IECON 1993., International Conference on Industrial Electronics, Control, and Instrumentation*, vol. 2, pp. 1342–1346, 1993.

[26] H. Sira-Ramirez, "Nonlinear p-i controller design for switchmode dc-to-dc power converters," *IEEE Transactions on Circuits and Systems*, vol. 38, pp. 410–417, 1991.

[27] F. Garofalo, P. Marino, S. Scala, and F. Vasca, "Control of dc-dc converters with linear optimal feedback and nonlinear feedforward," *IEEE Transactions on Power Electronics*, vol. 9, pp. 607–615, 1994.

[28] S. Sanders, G. Varghese, and D. Cameron, "Nonlinear control laws for switching power converters," *25th IEEE Conference on Decision and Control, 1986*, vol. 25, pp. 46–53.

[29] J. Ciezki and R. Ashton, "The design of stabilizing controls for shipboard dc-to-dc buck choppers using feedback linearization techniques," *Power Electronics Specialists Conference. PESC 1998 Record. 29th Annual IEEE*, vol. 1, pp. 335–341, 1998.

[30] I. Kondratiev, E. Santi, R. Dougal, and G. Veselov, "Synergetic control for dc-dc buck converters with constant power load," *Power Electronics Specialists Conference. PESC 2004. 2004 IEEE 35th Annual*, vol. 5, pp. 3758–3764, 2004.

[31] A. Khaligh, A. Rahimi, and A. Emadi, "Modified pulse-adjustment technique to control dc/dc converters driving variable constant-power loads," *IEEE Transactions on Industrial Electronics*, vol. 55, pp. 1133–1146, 2008.

[32] J. C.Wiseman and B.Wu, "Active damping control of a high-power pwm current-source rectifier for line-current thd reduction," *IEEE Transactions on Industrial Electronics*, vol. 52, pp. 758–764, 2005.

[33] L. Xinyun, A. Forsyth, and A. M. Cross, "Negative input-resistance compensator for a constant power load," *IEEE Transactions on Industrial Electronics*, vol. 54, pp. 3188–3196, 2007.

[34] P. Cancelliere, V. D. Colli, R. D. Stefano, and F. Marignetti, "Modeling and control of a zero-current-switching dc/ac current-source inverter," *IEEE Transactions on Industrial Electronics*, vol. 54, 2007.

[35] Z. Xie and H. Guo, "Stability analysis of synchronous generator-rectifier system with constant power loads," *Power Engineering and Automation Conference (PEAM), 2011 IEEE*, vol. 1, pp. 15–17, 2011.

[36] A. Jusoh, "The instability effect of constant power loads," *Power and Energy Conference. PECon 2004. Proceedings. National*, pp. 175–179, 2004.

[37] W. Weaver and P. Krein, "Implementing power buffer functionality in a dc-dc converter by geometric control," *Industry Applications Conference. 41st IAS Annual Meeting. Conference Record of the 2006 IEEE*, vol. 5, pp. 2529–2536, 2006.

[38] A. Rahimi and A. Emadi, "An analytical investigation of dc/dc power electronic converters with constant power loads in vehicular power systems," *IEEE Transactions on Vehicular Technology*, vol. 58, pp. 2689–2702, 2009.

[39] R. Erickson, "Optimal single resistors damping of input filters," *Applied Power Electronics Conference and Exposition. APEC 1999. Fourteenth Annual*, vol. 2, pp. 1073–1079, 1999.

[40] V. Vlatkovic, D. Borojevic, and F. Lee, "Input filter design for power factor correction circuits," *IEEE Transactions on Power Electronics*, vol. 11, pp. 199–205, 1996.

[41] S. Glover and S. Sudhoff, "An experimentally validated nonlinear stabilizing control for power electronics based power systems," *Society of Automotive Engineers, Inc.*, June 1999.

[42] S. Kelkar and F. Lee, "Adaptive input filter compensation for switching regulators," *IEEE Transactions on Aerospace and Electronic Systems*, vol. AES-20, pp. 57–66, 1984.

[43] A. Rahimi and A. Emadi, "Discontinuous-conduction mode dc/dc converters feeding constant-power loads," *IEEE Transactions on Industrial Electronics*, vol. 57, pp. 1318–1329, 2010.

[44] S. Huddy and J. Skufca, "Amplitude death solutions for stabilization of dc microgrids with instantaneous constant-power loads," *IEEE Transactions on Power Electronics*, vol. 28, pp. 247–253, 2013.

[45] D. Vilathgamuwa, X. Zhang, J. S.D.G, B. Bhangu, C. Gajanayake, and K. Tseng, "Virtual resistance based active damping solution for constant power instability in ac microgrids," *IECON 2011 - 37th Annual Conference on IEEE Industrial Electronics Society*, pp. 3646–3651, 2011.

[46] Q. Guan, P. Yang, X. Wang, and X. Zhang, "Stability analysis of matrix converter with constant power loads and lc input filter," *Power Electronics and Motion Control Conference (IPEMC), 2012 7th International*, vol. 2, pp. 900–904, 2012.

[47] A. Rahimi, "Addressing negative impedance instability problem of constant power loads: comprehensive view encompassing entire system from the load to the source," Ph.D. dissertation, Illinois Institute of Technology, 2008.

[48] K. Chaijaroenudomrung, K. Areerak, and K. Areerak, "The stability study of ac-dc power system with controlled rectifier including effect of voltage control," *European Journal of Scientific Research*, vol. 64, pp. 463–480, 2011.

[49] ——, "The controller design of three-phase controlled rectifier using an artificial intelligence technique," *European Journal of Scientific Research*, vol. 62, pp. 410–425, 2011.

[50] A. Ghosh and M. Kandpal, "State-space average modeling of dc-dc converters with parasitic in discontinuous conduction mode (dcm)," Ph.D. dissertation, National Institute of Technology, Rourkela, 2010.

[51] "Rotating (d-q) transformation and space vector modulation basic principles," *http://scholar.lib.vt.edu/theses/available/etd-031899-212402/unrestricted/APPENDIXES.PDF*.

[52] K. Chaijarurnudomrung, K.-N. Areerak, and K.-L. Areerak, "Modeling of three-phase controlled rectifier using a dq method," *International Conference on advances in Energy Engineering (ICAEE), 2010*, pp. 56–59, 2010.

[53] C.-M. Ong, *Dynamic Simulation of Electric Machinery using Matlab and Simulink*, 1998.

[54] "http://www.mathworks.com/help/control/ref/lqr.html."

[55] J. Hespanha, "Lqg/lqr controller design," April 2007.